Ontogenetic changes in shape and growth rate during postnatal development in false killer whales (Pseudorca crassidens) vertebral column

Duflot, Mélissa L.; Gillet, Amandine; Jones, Katrina E.; Sabin, Richard; Lanzetti, Agnese

Link to publication on Research at Birmingham portal

ARTICLE

Marine Mammal Science

Ontogenetic changes in shape and growth rate during postnatal development in false killer whales (*Pseudorca crassidens*) vertebral column

Mélissa L. Duflot[1,2] | **Amandine Gillet**[3,4] |
Katrina E. Jones[3] | **Richard Sabin**[2] | **Agnese Lanzetti**[5,6]

[1]Centre for Biodiversity and Environment Research Department of Genetics, Evolution and Environment, University College London, London, UK

[2]Department of Life Sciences, Natural History Museum, London, UK

[3]School of Natural Sciences, Department of Earth and Environmental Sciences, University of Manchester, Manchester, UK

[4]Museum of Comparative Zoology and Department of Organismic and Evolutionary Biology, Harvard University, Cambridge, MA

[5]Department of Geography, Earth and Environmental Sciences, University of Birmingham, Birmingham, UK

[6]Imaging and Analyses Centre, Natural History Museum, London, United Kingdom

Correspondence

Agnese Lanzetti, Imaging and Analyses Centre, Natural History Museum, Cromwell Road, SW7 5BD, London, UK.
Email: agnese.lanzetti@gmail.com

Funding information

Horizon 2020 Framework Programme; European Commission, Grant/Award Number: 894584

Abstract

Intraspecific variation in cetacean vertebral anatomy as a result of ageing, growth, and sexual dimorphism is poorly understood. Using 3D geometric morphometrics, we investigated allometric patterns, sexual dimorphism, and ontogenetic trajectories in the vertebral column of false killer whale (*Pseudorca crassidens*). Our data set includes thoracic, lumbar, and caudal vertebrae of 30 specimens, including neonates, juveniles, and adults of both sexes. Vertebral shape was significantly correlated with size within each region. Neonatal vertebral shape differed significantly from juveniles and adults, displaying ontogenetic shape change. Allometric and growth patterns of the vertebral regions, particularly of the lumbar region with the thoracic and caudal regions, differed significantly, which may influence the function and mobility patterns of the vertebral regions during different life stages. Using quantitative methods, we could not conclude that the *Pseudorca* vertebrae are sexually dimorphic. This study describes for the first time intraspecific vertebral patterns in a cetacean species across ontogenetic stages. *Pseudorca* individuals live in large pods and swim together, sharing the same swimming mode. The neonates have a more flexible column and swim less efficiently following their mothers to nurse.

1 | INTRODUCTION

Research in cetaceans' skull allometry and ontogeny is advancing (e.g., del Castillo et al., 2017; Galatius et al., 2011); however, sexual dimorphism and ontogenetic allometry—the statistical relationship between shape and size during growth (Klingenberg, 1996)—in the postcranial skeleton for most cetacean species remain overlooked (Marchesi et al., 2021). The vertebral column supports the body and provides flexibility and mobility to propel through the water (Buchholtz, 2001; Fish et al., 2003) and different vertebral regions contribute to unique functions (Buchholtz & Schur, 2004). Modern cetacean vertebral regions are identified as follow: the cervical consists of a block of seven cervical vertebrae with varying level of fusion lacking rib attachment, the thoracic is made of rib-bearing vertebrae, the lumbar starts directly after the thoracic region and includes vertebrae lacking a rib attachment, the caudal comprises vertebrae bearing chevron bones on the ventral facet of the vertebral centrum with some vertebrae having laterally compressed centra, the last few dorso-ventrally compressed vertebrae are part of the fluke (Rommel, 1989). A rounded vertebra, known as the "ball vertebra"; is sometimes identified at the transition between the laterally compressed vertebrae of the peduncle and the dorsoventrally compressed vertebrae of the fluke (Watson & Fordyce, 1993). The cetaceans' vertebral regionalization reflects their axial locomotion with a vertebral column that moves along a sagittal plane with restricted rotation (Buchholtz & Schur, 2004). Changes in the relationship between shape and size between postcranial elements affect the swimming mode of cetaceans during development (Noren et al., 2006). However, such research on cetacean vertebral development and intraspecific variation is lacking (Marchesi et al., 2021).

In this work, we studied the development and sexual dimorphism of the vertebral series of the false killer whale (*Pseudorca crassidens*) following this regionalization pattern excluding the cervical and fluke regions. The vertebral formula of *Pseudorca* is C7-T10-L10-11-Ca22-23, with no more than 53 vertebrae in total (Yamada, 1956). Previous work described the *Pseudorca* vertebrae with shortened centrum throughout the posterior caudal region forming a unified rigid peduncle (Buchholtz, 2001). This rigid peduncle provides support for oscillatory movement. In the rest of the column, vertebral centra remain elongated, providing more flexibility (Buchholtz, 2001). Short-finned pilot whales (*Globicephala macrorhynchus*), pygmy killer whales (*Feresa attenuata*), melon-headed whales (*Peponocephala electra*), and *Pseudorca*, among other delphinids, exhibit sexually dimorphic traits in body proportions, fin (Rone & Pace, 2012; Yahn et al., 2019), and head (Kitchener et al., 1990; Mead, 1975), facilitating sex determination (Yahn et al., 2022). *Pseudorca*, with a maximum male length of 5.96 m and a maximum female length of 5.06 m (Yamada, 1956) is one of the largest delphinids (Baird, 2018; Stacey et al. 1994). At birth, *Pseudorca* measures 1.5 to 2.1 m long; females reach sexual maturity at 8–11 years old, whereas males reach sexual maturity about 8–10 years after females. Mead (1975) reported sexual dimorphism in the appearance of the head, more specifically in the melon. Overall, the skull and teeth of males are larger than those of females (Kitchener et al., 1990). The recent 3-dimensional (3D) geometric morphometric analysis of *Pseudorca* skulls confirmed that males and females are sexually dimorphic in size but not in shape (Vicari et al., 2022).

Similarly to the two pilot whales (*G. macrorhynchus* and *G. melas*), *Pseudorca* displays a unique social bond. It lives in large mixed pods with males, females, young, and adults together, and occasionally strands en masse, with the largest ever recorded mass-stranding event comprised of 835 individuals (Baird, 2018). Though unfortunate, these mass-stranding events provide unique opportunities for scientists to understand these rare species, especially using advanced morphological analysis (Coombs et al., 2019). Recent studies on the development of the vertebral column of Delphinidae were restricted to four dolphin species of the Lissodelphininae subfamily, namely the Commerson's dolphin (*Cephalorhynchus commersonii*), dusky dolphin (*Lagenorhynchus obscurus*), hourglass dolphin (*Lagenorhynchus cruciger*), and Peale's dolphin (*Lagenorhynchus australis*) (Marchesi et al., 2021). These are smaller and mostly solitary

species (Marchesi et al., 2021), therefore do not represent a good model to understand growth and dimorphism of highly social taxa.

As a result, the purpose of this study was to add to this limited body of knowledge, namely to delphinid vertebral ontogeny and sexual dimorphism, using 3D geometric morphometric analysis and a novel statistical approach. Specifically, focusing on the false killer whale, we address the following questions: (1) How does the shape of the vertebrae relate to size? (2) What is the level of morphological variation in the column through ontogeny? (3) Is the vertebral column sexually dimorphic in shape and size?

Based on previous work, we predicted that allometry (growth rate) would significantly affect the vertebral morphology (hypothesis 1), the column morphology would vary among age groups (hypothesis 2; Marchesi et al. 2021), and the vertebrae would be sexually dimorphic in size but not in shape (hypothesis 3; Vicari et al. 2022).

2 | METHODS

2.1 | Specimens

We sampled a total of 30 specimens conserved at the Natural History Museum, London, UK (Table S1). All the specimens came from the same mass-stranding event that occurred at the Dornoch Firth, Scotland, in 1927. Most specimens' epiphyses were detached, therefore, we did not include the epiphyses and concluded that the degree of fusion of the vertebral epiphyses was not an indicator of sexual maturity for this collection as already established in Yamada (1956). Even though the absolute age of each individual was unknown because it was not recorded at the time of the stranding, we could classify them into different age classes, namely, neonate, juvenile, and adult based on total body length measurements. Male *Pseudorca* are considered adults when measuring more than 435 cm, whereas females are considered adults when measuring more than 382 cm (Yamada, 1956). Therefore, males measuring less than 435 cm and females measuring less than 382 cm were considered juveniles. We distinguished the two neonates based on the sutures of their skulls and their total body length, which was <285 cm. We scanned the vertebrae of six juvenile males (with a total body length ranging from 330.2 cm to 434.34 cm) and nine adult (with a total body length ranging from 472.44 cm to 568.96 cm) males, and three juvenile females (with a total body length ranging from 320.04 cm to 430.53 cm) and eight adult (with a total body length ranging from 431.8 cm to 477.52 cm) females. We also scanned the two neonates (one male and one female, measuring 243.54 cm and 286.56 cm), as well as two juveniles of unknown sex and total length. We assigned these two specimens to the juvenile age class based on the similar vertebral and skull size to other specimens in the data set.

In total, 434 vertebrae, including 104 thoracics, 144 lumbars, and 179 caudals were surface scanned and digitized using a Creaform Go!SCAN20 or a Creaform Go!SCAN50 depending on the size of the vertebrae. When choosing which specimens and vertebrae to surface scan, we selected the most complete specimens with collection information such as total length and sex, and representative of the full age range including the smallest and biggest complete specimens. We did scan some cervical blocks but did not conduct analyses on them as in many cases C5-C6-C7 were missing. We did not include dorsoventrally compressed fluke vertebrae in the analyses as they are often missing from collections or unreliably assigned, and only scanned anteroposteriorly compressed caudal vertebrae. The scans were merged in VX Elements v6.0 and then exported in obj format. They were then cleaned and decimated down to 550,000 triangles in Geomagic Wrap software (3D Systems). The holes in the vertebral models were also filled in Geomagic Wrap (3D Systems) and they were exported in ply format ahead of landmarking.

2.2 | Morphometric data collection

The lumbar, thoracic, and caudal regions in cetaceans differ, thus, we opted for a different landmarking scheme for the vertebrae of each region (Randau et al. 2016). We landmarked the centra and processes of all vertebrae

(Figure S1). We placed 16 (thoracic and lumbar) and 13 (caudal) anatomically defined landmarks over the surface of the vertebrae in Stratovan Checkpoint (Stratovan, Davis, CA) using single points (landmarks) in addition to curves (semilandmarks; Table S1). We placed 10 landmarks on the right-hand side of the thoracic, and 6 landmarks on the midline, 16 landmarks covered the dorsal and ventral face of the thoracic vertebrae. We placed 8 landmarks on the right-hand side of the lumbar, and 8 landmarks on the midline; 16 landmarks covered the dorsal and ventral face of the lumbar vertebrae. We placed 8 landmarks on the right-hand side of the caudal, and 5 landmarks on the midline; 13 landmarks covered the dorsal and ventral face of the caudal vertebrae. In order not to overrepresent more complete specimens and have an even sample size, we selected the most complete three thoracics, four lumbars, and five caudals to be used in the following analyses. We made sure that the vertebrae selected were evenly distributed along the length of each region (i.e. the three thoracic vertebrae selected roughly corresponded to the anterior, the mid, and the posterior thoracic). One caudal vertebra for specimen C-1961-6-14-12 was used twice as only four suitable vertebrae were available.

Some specimens have missing data, however, for geometric morphometric analyses and using the plotting functions in the "geomorph" R package v4.0.6 (Adams et al., 2021), the full scheme of landmarks is needed (Adams et al.,2021). The "missing" landmark can be imputed by using the "non-missing" landmarks to estimate its positions (Coombs et al. 2020). The missing landmark is an area that cannot be digitized (i.e., when a piece of bone is missing), therefore, to estimate its position, we placed the missing landmarks on the surface of the vertebrae that misses a piece of bone, and marked it as missing landmark in Checkpoint. Then, Checkpoint automatically assigns the coordinate -9999 to the missing landmarks. Following this, we used the *fixLmtps* function in the package Morpho v2.11 (Schlager, 2017) to evaluate the position of landmarks on broken, incomplete, or unossified specimens. Using this function, a reference vertebra with complete set of landmarks was selected, on which the incomplete vertebrae were aligned. This alignment allowed the missing landmarks to be imputed on the incomplete vertebrae. Semilandmark curves were resampled to a consistent number of points (4–10 points depending on the curve) for each curve and slid on the surface to ensure homology among points using a customized *slider3d* function the package Morpho (Bardua et al., 2019). Since we only recorded the right-hand side of the vertebrae of each specimen, afterwards, we created mirrored landmarks and curves for the left-hand side using the *mirrorfill* function in the "paleomorph" R package v0.1.4 (Lucas & Goswami, 2017) to ensure correct alignment of specimens. All code used for preparing and analyzing the data as discussed below is available on GitHub (https://github.com/AgneseLan/false-killer-column; https://doi.org/10.5281/zenodo.10829622)

2.3 | Data analysis

2.3.1 | Morphospace of vertebrae

Analyses were conducted in R (R Core Team, 2021) using the "geomorph" package v4.1.0 (Adams et al. 2021). The landmarks coordinates were aligned with Generalized Procrustes superimposition (GPA) using the *gpagen* function. Analyses were conducted on the three types of vertebrae separately (thoracic, lumbar, caudal) of all the specimens together. Principal component analysis (PCA) was used to quantify vertebral shape variation per type of vertebrae separately using the *gm.prcomp* function. Shape variation was visualized on the main axes for each vertebral region with mesh warping using the 3D mesh of the mean vertebra.

The vertebral column of cetaceans functions as a whole, therefore, we wanted to align all vertebrae to analyze them together as an entire column, rather than separately. Because the vertebral shape varies significantly along the column and we used a different landmark configuration to characterize each of the three regions, we could not simply align all vertebrae using a standard GPA. Instead, we conducted a multi-block analysis using the "morphoBlocks" package v0.1.0 (Thomas et al. 2021). Using the landmarks and semilandmarks even in different configurations, this package created a multiple part morphospace with a regularized consensus principal component analysis (RCPCA)

(Thomas et al., 2021). All the vertebrae scanned could not be used, because the package requires the same number of vertebrae per specimen per region to be analyzed. For each individual, we used the most complete vertebrae available, making sure to include morphological and size variation in each region. We had to cut down the number of vertebrae as the samples need to be the same number across all blocks. Therefore, one lumbar and two caudals were cut from the data set for each specimen, leaving three vertebrae per type per specimen. Data blocks (one for each vertebra type) were generated, combined, and aligned to visualize and analyze these vertebrae in the same morphospace. After a common GPA alignment, a RCPCA was then performed using the *rgcca* function from the "RGCCA" package (Tenenhaus & Guillemot, 2017) under the *analyseBlocks* function. This method produces a dimensionality reduction analogous to a traditional PCA analysis. The scores obtained from the RCPCA were then exported and used to perform all subsequent analyses of the relationship of vertebral shape and size, sex, and age (Felice et al. 2019).

Correlation between PC1 and PC2 and major traits such as size, sex, and age were tested for both the traditional PCA and the RCPCA using the *lm* function in base R.

2.3.2 | Vertebral allometric patterns

To test the change in shape and growth rate between the vertebrae (Q1, hypothesis 1), we performed linear regressions using the PC scores extracted from the RGPCA to represent the shape of the vertebrae in each region and size summarized as log10-transformed centroid size of the vertebrae using the *lm.rrpp* function from the "RRPP" R package v1.1.2 which uses a residual randomization permutation procedure (Collyer & Adams, 2021). A combination model was used to explore the effect of the grouping on the overall shape but not the rate of change. While the interaction model explored the effect of grouping on the overall shape and growth rate. Models were compared using the *anova* function in base R, and we found that the interaction model was the best supported compared to null model with no differences in allometry between vertebra types and the combination model ($Z = 7.6451$, $p = .001$). We used *pairwise* in the package "RRPP" to test pairwise differences between the slopes which represented the differences in growth rate between vertebral regions.

2.3.3 | Effect of sexual grouping on vertebral shape and size

The effect of sex grouping on vertebral shape was quantitatively tested by running ANOVAs using the *lm.rrpp* and *pairwise* functions from the "RRPP" package. The effect of sex grouping on vertebral size was also quantitatively tested by running ANOVAs using the same functions as above with log10 centroid size as proxy for vertebral size. We also tested the sexual dimorphism in each vertebra type separately to confirm our results obtained with the multiblock analysis.

2.3.4 | Trajectory analysis

We assessed the variation of vertebral shape along the column with phenotypic trajectory analyses using the *trajectory.analysis* function from the "geomorph" R package (Collyer and Adams (2013). Two analyses were run using the morphoblocks PC scores: one comparing trajectories at different growth stages and another comparing trajectories among sexes. Trajectory analyses to compare growth pattern between the sexes were also conducted on the separately aligned vertebral regions. The *trajectory.analysis* function allowed us to test pairwise differences in trajectories shape, length, and direction from the thoracic to lumbar to caudal between neonates, juveniles, and adults (Q2, hypothesis 2) and then between males and females (Q3, hypothesis 3).

3 | RESULTS

3.1 | Morphospace of vertebrae

In the morphospace obtained by aligning the vertebrae as separate morphoblocks (thoracic, lumbar, and caudal), PC1 accounts for 33.55% of the total variance, and PC2 accounts for 6.57% of the total variance (Figure 1). PC1 was associated with age (p = <2.2e-16) and size (p = <2.2e-16), and weakly with sex (p = .04528). For all three types of vertebrae, the centrum became more elongated, the neural processes became wider and shorter, and the apophyses also increased in width during growth, along with an increase in size, from the positive to the negative side of the axes. PC2 was associated only with size (p = 7.708e-06). The centrum increased in length slightly and the neural process became more posteriorly bent going from the negative to the positive side of the axis. This was accompanied by an increase in size and ontogenetic age. Neither the age groups nor the sexes could be parsed out by the PCA, with their ranges overlapping significantly (Figures 1 and S2). Even when analyzing the three types of vertebrae separately, namely, for thoracic (Figure S3), lumbar (Figure S4), and caudal (Figure S5), there was a large overlap between sexes and age groups in all three morphospaces.

3.2 | Vertebral allometric patterns

Linear regressions highlighted a significant positive allometric relationship between the size and shape of the verte-brae, with distinct patterns distinguishing thoracic, lumbar, and caudal vertebrae (Figure 2). The pairwise comparisons
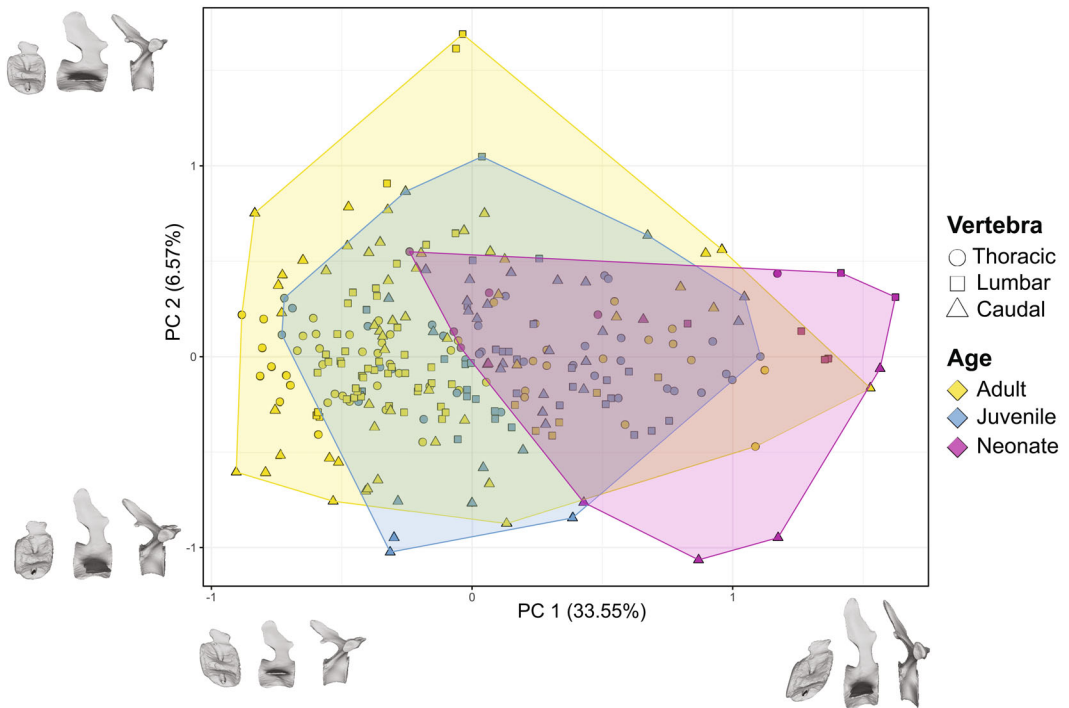
FIGURE 1 Principal components analysis plot of PC1 against PC2 calculated on adult (yellow), juvenile (blue), and neonate (Tyrian purple) age groups for the different vertebrae thoracic, lumbar, and caudal. PC1 explains 33.55% of the variance, based on centrum length and processes width. PC2 explains 6.57% of the variance also based on centrum length and spinal process angle. Convex hulls represent the different age groups: adult (yellow), juvenile (blue), neonate (Tyrian purple).

FIGURE 2 Allometry of shape (regression score) relative to the logarithm of centroid size by vertebral (thoracic: green, solid line; lumbar: orange, dashed line; caudal: lilac, dotted line) and age groups (● adult, ■ juvenile, and ▲ neonate). Model fit: $R^2 = 0.1719$, $p = .001^*$.

TABLE 1 Summary of results for pairwise comparisons of allometric models of size for the three types of vertebrae.
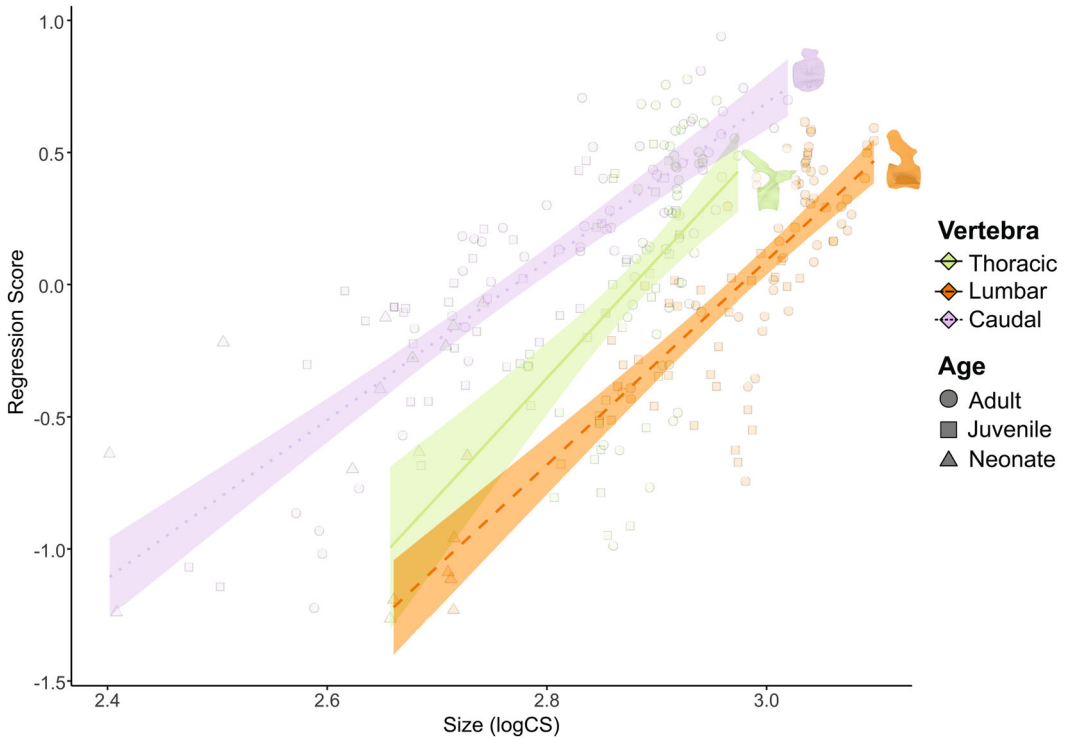
Absolute slopes difference (growth rate)	Difference	Z-scores	p-values
Thoracic:Lumbar	2.403	1.721	.043*
Thoracic:Caudal	2.072	1.374	.088
Lumbar:Caudal	1.762	1.857	.031*
Distance between slopes angles (direction of growth)	Angle	Z-scores	p-values
Thoracic:Lumbar	30.981°	1.269	.099
Thoracic:Caudal	25.574°	0.837	.201
Lumbar:Caudal	19.475°	0.847	.200
Difference between lengths (length of growth)	Difference	Z-scores	p-values
Thoracic:Lumbar	0.010	−2.203	.991
Thoracic:Caudal	1.169	1.495	.066
Lumbar:Caudal	1.179	2.074	.009*

Note: Significant *p*-values highlighted with an asterisk.

showed a significant difference in the growth rate between the lumbar vertebral region with the thoracic and caudal vertebral regions, but no difference was detected between thoracic and caudal regions (distance of slopes), partly supporting hypothesis 1 (Table 1). None of the vertebrae (thoracic, lumbar, and caudal) direction of growth (angles of

slopes) differed significantly, this result is depicted by almost parallel regression lines (Figure 2). The caudal region had the longest growth slope, with it being significantly different than the lumbar slope (Table 1).

3.3 | Effect of sexual grouping on vertebral shape and size

The global morphospace from morphoblocks highlighted a large overlap between sex groups (Figure S2). Similar patterns were observed when plotting each vertebral region separately, no shape difference could be identified between females and males for the thoracic (Figure S6), lumbar (Figure S7), and caudal (Figure S8) vertebrae.

When considering each vertebral type separately across all *Pseudorca* sex groups, the vertebral shape did not vary significantly between sexes, either when conducting the ANOVA on the morphoblock-aligned vertebrae considering the interaction between vertebra type and sex, and when considering the different vertebrae separately (Table 2). Furthermore, we did not find a significant difference in the vertebral size between females and males *Pseudorca* when vertebrae were analyzed separately (Table 2). A significant difference was found when the vertebrae were analyzed together in morphoblock, but the difference was not recovered when performing the pairwise analysis (absolute difference $p = .174$). The significance is likely driven by the difference in size among vertebrae types rather than between sexes ($Z = 8.137$, $p = .001$). Although part of hypothesis 3 expected sexual size dimorphism, the results suggests that there may be a lack of both shape and size dimorphism. The vertebrae of *Pseudorca* may not be sexually dimorphic.

3.4 | Trajectory analysis

On the PCA projection, the plotted trajectories depicted the shape variation along the column at each developmental stage and highlighted a vertebral shape variation along the column of the neonates compared to more mature individuals (juveniles and adults) (Figure 3). The neonate specimens have higher PC1 values than the more mature specimens. It corresponds to shorter vertebral centra and narrower processes. Patterns of vertebral shape change along the column of *Pseudorca* varied significantly among age classes (trajectory analysis fit: $p = .001$), corroborating hypothesis 2. Indeed, a pairwise difference of phenotypic trajectories along the column through ontogeny showed a significant difference in the length of the trajectories between adults and neonates and juvenile and neonates. Adults

TABLE 2 Summary of results for ANOVA analyses of vertebrae shape and size differences between females and males.

	Z-score	p-value
Shape		
Morphoblocks	−1.940	0.977
Thoracic	0.771	0.229
Lumbar	0.559	0.296
Caudal	0.524	0.315
Size		
Morphoblocks	8.721	0.001*
Thoracic	0.885	0.209
Lumbar	0.438	0.362
Caudal	1.161	0.127

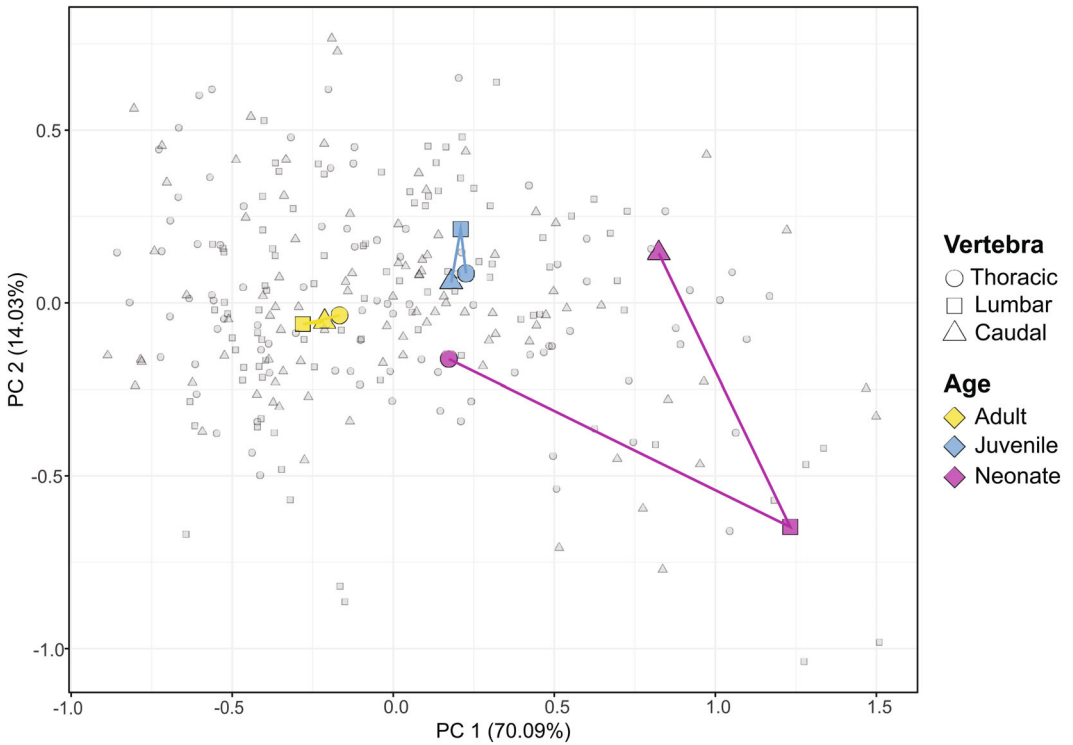*Note*: Significant *p*-values highlighted with an asterisk.

FIGURE 3 Trajectories of change in shape on the first two principal components (PC) axes during ontogeny of *Pseudorca* for the ● thoracic, ■ lumbar, and ▲ caudal. Age classes: adult (yellow), juvenile (blue), neonate (Tyrian purple). PC1 explains 70.09% of the variance, PC2 explains 14.03% of the variance.

TABLE 3 Summary of results for pairwise trajectory shape analyses of the backbone through ontogeny.

Length of trajectory	Difference	Z-scores	p-values
adult:juvenile	0.118	0.298	.390
adult:neonate	2.012	4.845	.001*
juvenile:neonate	1.894	4.334	.001*
Direction of trajectory	**Angle**	**Z-scores**	**p-values**
adult:juvenile	124.939°	1.561	.059
adult:neonate	130.453°	1.784	.026*
juvenile:neonate	100.652°	0.478	.354
Shape of trajectory	**Difference**	**Z-scores**	**p-values**
adult:juvenile	0.188	−0.587	.713
adult:neonate	0.021	−2.523	.996
juvenile:neonate	0.175	−0.722	.754

Note: Significant p-values are indicated with an asterisk.

and neonates also differed in the direction of the trajectory (Table 3). Adults and juveniles overall displayed a more uniform vertebral shape throughout the column, while the longer trajectory in neonates indicates more marked regionalization.

When analyzing the shape variation along the column of males in comparison to females excluding two juveniles of unknown sex in the records (Figure 4), the male specimens had similar PC1 and PC2 values to the female specimens. Patterns of vertebral shape change along the column of *Pseudorca* were not found to vary significantly between males and females (trajectory analysis fit: $p = .688$), supporting hypothesis 3. Indeed, the pairwise comparison of phenotypic trajectories along the column between sexes confirmed this result because no difference in the length, direction, or shape of the trajectories was detected between males and females (Table 4).

We analyzed the three types of vertebrae separately to check if there was a difference in growth trajectory between the sexes, to highlight potential developmental differences. For the thoracic vertebrae, no significant differences were found in any aspect of the growth trajectories (Figure S8, Table S3). For the lumbar (Figure S9) and
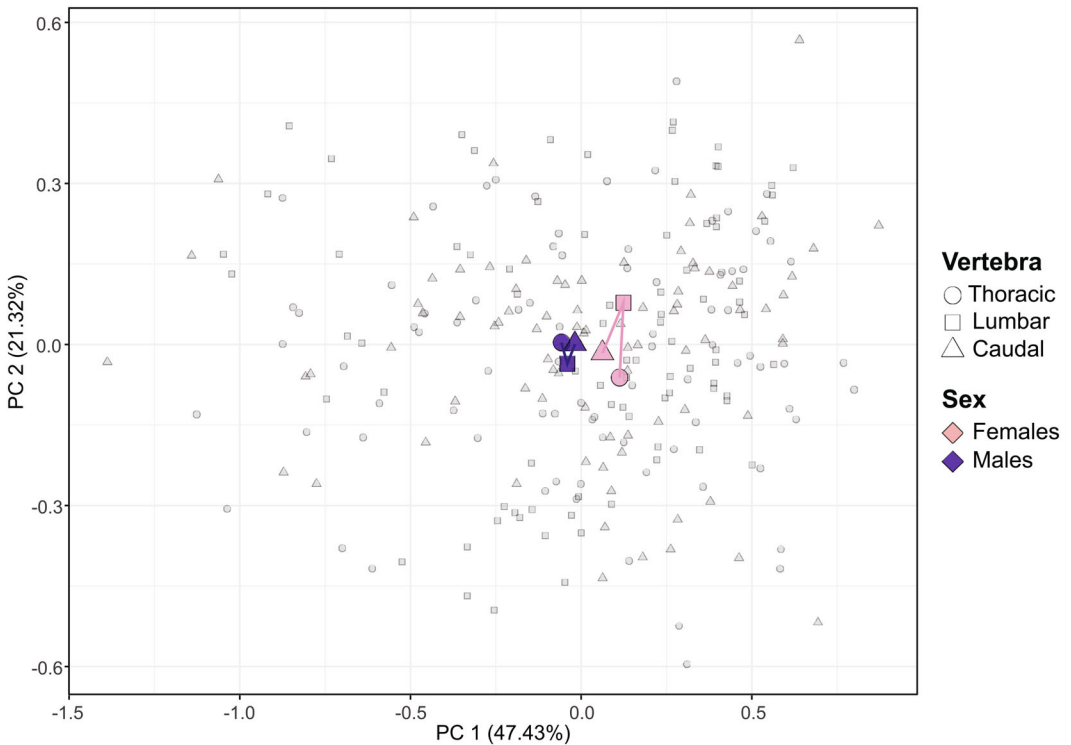

FIGURE 4 Trajectories of change in shape on the first two principal components (PC) axes of *Pseudorca* for the ● thoracic, ■ lumbar, and ▲ caudal vertebrae. Sexes: female (pink), male (dark blue), excluding the juveniles of unknown sex. PC1 explains 47.43% of the variance, PC2 explains 21.32% of the variance.

TABLE 4 Summary of results for pairwise comparisons of sex-related shape trajectories.

Length of trajectory	Difference	Z-scores	p-values
Female:Male	0.137	0.678	.261
Direction of trajectory	**angle**	**Z-scores**	**p-values**
Female:Male	129.560°	0.451	.354
Shape of trajectory	**Difference**	**Z-scores**	**p-values**
Female:Male	0.191	−0.627	.730

Note: Significant *p*-values are indicated with an asterisk.

caudal (Figure S10), only marginal differences were found in the shape and length of the trajectory respectively (Table S3).

4 | DISCUSSION

4.1 | Vertebral allometry: the false killer whales thoracic, lumbar and caudal vertebrae differed in growth rate

We examined intraspecific vertebral allometry in the false killer whale and found a significant positive relationship between the vertebral size and change in shape. In particular, we found a positive allometry of size and shape is shared by the vertebrae (Figure 2), with significant differences in allometry and shape between the lumbar region and thoracic and caudal regions (Table 1).

Lumbar vertebrae have a tall flat-surfaced centrum and tall processes akin to other cetaceans (Buchholtz & Schur, 2004; Marchesi, Mora, et al., 2020). Their neural processes are the point of origin of the epaxial muscle, which inserts onto caudal vertebrae (Pabst, 1990). Therefore, having long processes could improve the lever arm efficiency while also providing a large attachment point for the caudal tendon (Buchholtz & Schur, 2004). This could provide a mechanical advantage by facilitating the upward movement of the caudal region (Marchesi et al., 2021; Pabst, 1990). Large apophyses can also help stabilizing this region of the column which could provide the propelling force necessary to swim (Buchholtz & Schur, 2004).

The anterior thoracics of *Pseudorca* are disc-shaped with small processes, the posterior thoracics that transition into the lumbar vertebrae grow a spool-shaped centrum. The thoracic region usually helps the cervicals in supporting the head and limits pitching induced by the propelling force from the torso (Fish et al., 2003; Marchesi, Mora, et al. 2020). The region also provides attachment for the ribs and assists with breathing while swimming (Cotten et al., 2008). *Pseudorca* is known to perform wide turns while swimming (Fish et al., 2003), reflecting constrained maneuverability which could arise from a combination of disc-shaped vertebrae and rib attachment in the thoracic region.

The anterior caudals transition from the lumbars to the laterally compressed caudals and are spool-shaped with short processes. However, the rest of the region has laterally compressed centra with convex anterior and posterior faces. These latter ones allow rotation and high vertical displacement (Buchholtz & Schur, 2004). Therefore, while the anterior caudals could help provide propelling force with the lumbars (Buchholtz & Schur, 2004), the compressed and convex caudals could possibly be related to the oscillatory movement of the fluke (Buchholtz, 2001). In fact, this may reflect the locomotor pattern categorized as carangiform with lunate-tail swimming, a characteristic of some of the fastest marine vertebrates, including cetaceans (Lang & Daybell, 1963; Lighthill, 1969; Videler & Kamermans, 1985). Indeed, Fish (1998) previously found that *Pseudorca* exhibited a high coefficient of drag and efficiency, indicating adaptations that may benefit the pursuit of large and fast-swimming prey. The combination of low sweep with high aspect ratio, previously observed in *Pseudorca*, was associated with high-efficiency rapid swimming, while variations in sweep compensated for lift production, influencing thrust (Fish, 1998) which seems to concur with our results.

Overall, these morphological changes along the column suggest different function of each region which are probably related to the locomotion of *Pseudorca*. However, the swimming biomechanics of this species are not well understood.

4.2 | The difference in false killer whale's column morphology leads to swimming mode changes through ontogeny

Recently, marine mammal anatomists have started to focus their studies on the vertebral morphology of cetaceans (Buchholtz & Schur, 2004; Gillet et al., 2019; Marchesi, Boy, et al., 2020; Marchesi, Mora, et al. 2020). However, only

one described the ontogenetic trajectories of cetaceans, namely of the Commerson's dolphin (*Cephalorhynchus commersonii*), dusky dolphin (*Lagenorhynchus obscurus*), hourglass dolphin (*Lagenorhynchus cruciger*), and Peale's dolphin (*Lagenorhynchus australis*) (Marchesi et al., 2021). As the first study to investigate the vertebral ontogenetic trajectories of a Globicephalinae species, we found a significant difference in the direction of the column trajectories through ontogeny. All three vertebral regions of the neonates' column differed from those of the juveniles and adults (Figure 3, Table 3). In particular, the neonates vertebral shape change differed significantly from adults and juveniles, and the vertebral length trajectory differed among all age groups. Though, as a whole, vertebral morphologies broadly overlap across ages, not allowing for age determination just by using these bones in isolation (Figure 1).

As we hypothesized, neonates' vertebral column traits differ significantly from adults. Indeed, the neonates have spool-shaped vertebrae with short processes along the column, suggesting that most of the column is flexible (Buchholtz & Schur, 2004). This finding contrasts the small terrestrial mammal's growth patterns, these mammals are born with short disc-shaped centra which develop into more elongate ones (Jones & German, 2014). Without any stability in the column, the *Pseudorca* neonates would have limited propulsive efficiency and would swim less efficiently (Fish et al., 2003). In fact, neonate common bottlenose dolphins (*Tursiops truncatus*) were also found to swim slowly during their first year after birth and had a weaker thrust production with a low propelling force compared to adults (Noren et al., 2006). This inability to swim fast in bottlenose dolphin neonates could be extended to *Pseudorca* neonates, which have a significantly different vertebral column than juveniles and adults.

With little support provided by the thoracics, the neonates potentially have little control over their heads and would be at a disadvantage in prey searching (Fish et al., 2003). Females *Pseudorca* were estimated to lactate for approximately 18 months after giving birth (Kasuya & Izumisawa, 1981; Perrin & Reilly, 1984). Even though the lactation period is highly variable among cetacean species, based on their body size and anatomical features, it can be assumed that the neonates of our study were still very young and dependent on their mother's milk. The flexibility of the whole column, especially of the thoracic, allows the head to turn and would facilitate suckling underwater (Noren et al., 2006). Investigation of the cervical vertebrae would help confirm this assumption.

Finally, through ontogeny, a significant difference in the adults and neonates' trajectories direction was detected (Table 3). The vertebrae of cetaceans, similarly to terrestrial mammals, have three ossification centers (Bateman, 1954). These ossification centers are the vertebral centrum and the two vertebral arches. The vertebrae ossify in two stages: during the primary ossification, the three centers of ossification merge (Bateman, 1954). Then, during secondary ossification, the vertebral arches further ossify and expand outwards (Bateman, 1954). The differences in trajectory length and direction detected between those age groups may be attributed to the ossification of the vertebrae (Table 3). The neonates' first ossification phase was completed because all three ossification centers were merged (Bateman, 1954). However, the second stage of ossification was potentially not met, explaining differences in length and direction trajectories compared to adults (Bateman, 1954).

We acknowledge that the low number of neonates could influence the results of this study compared to juveniles and adults. However, these neonates were the best preserved in the collection. The study could be improved by adding complete neonate samples.

4.3 | False killer whales are not likely sexually dimorphic

Out of 93 extant species of cetaceans, no study on the sexual dimorphism of the vertebral column has been done previously. We are, therefore, the first to bring insights into the post-crania sexual dimorphism patterns. This study detected no difference in length and direction of the trajectories between males and females (Figure 4, Table 4) and no sexual shape and size differences in the vertebral column of *Pseudorca*. Even when analyzing the three types of vertebrae separately, no differences in shape and size were detected between males and females (Table 2). However, our samples sizes were small so we must be cautious and only suggest there is likely no sexual dimorphism.

The potential lack of sexual size dimorphism found is surprising because *Pseudorca* females usually reach sexual maturity 8–10 years before males (Stacey et al., 1994). By achieving sexual maturity before males, one could expect that females would be significantly smaller (Mesnick & Ralls, 2018); however, our findings did not seem to reflect this. Usually, smaller females can invest energy in completing gestation and nursing the calves, especially in Cetacea with a long gestation period like the *Pseudorca* which lasts up to 15.5 months (Purves & Pilleri, 1978). In contrast, males invest energy in growing larger to attract a mating partner (Mesnick & Ralls, 2018).

Sexual dimorphism in body size has been detected previously in a few other cetacean species, notably in the two most closely related species to *Pseudorca*, the long and short-finned pilot whales (*Globicephala* spp.; Mesnick & Ralls, 2018; Yahn et al., 2023). Larger anatomical features displayed by males were thought to serve various purposes, such as signaling to mates or competitors (Mesnick & Ralls, 2018), aiding maneuverability for social and intraspecific interactions (Mesnick & Ralls, 2018; Ngqulana et al., 2017), or contributing to thermoregulation (Tolley et al., 1995). Additionally, environmental conditions can influence the extent of dimorphism, with enhanced male features observed in more productive areas (Amano & Miyazaki, 1996; Bell et al., 2002). However, these studies did not use the column using a cutting-edge method, therefore, using more precise 3D geometric morphometric methods, we were able to establish the likely absence of sexual size dimorphism in the column/vertebrae of a Delphinidae species.

Pseudorca lives in large and mixed pods, with approximately the same number of males and females (Baird, 2018; Yamada, 1956). The previous lack of sexual shape dimorphism in the skull of the same *Pseudorca* population was assumed to reflect their social bond within the pod and cooperative hunting (Odell & McClune, 1999). Males and females share the same foraging strategy meaning they may not need to grow different skulls shape (Odell & McClune (1998). However, this is speculative and even though the lack of sexual shape dimorphism in the column/vertebrae between males and females could be related to their cooperative behavior, the main conclusion that can be drawn is that males and females have similar swimming mode.

With the potential presence of sexual dimorphism in skull size (Vicari et al., 2022), and melon (Mead, 1975) and the absence of shape and size dimorphism in the vertebral column, it may be assumed that the sexual size dimorphism in *Pseudorca* may be concentrated in the cranial area, or in other postcranial morphological traits that were previously studied as a whole (Yahn et al., 2023), whilst we focused on the single vertebrae, and too little to be detected in the backbone skeleton. Even though the possible lack of sexual dimorphism in shape could suggest that males and females have similar locomotion mode, the study was constrained to investigating allometric patterns and did not incorporate biomechanical or kinematic data. It would be of interest to conduct similar studies on other closely related species while incorporating functional data.

4.4 | Conclusions

Using 3D geometric morphometrics we found that vertebral shape was significantly influenced with size for each vertebral region. Neonatal column/vertebral shape differed from juveniles and adults, with shape change significantly different along the column through development. Allometric and growth rate of the vertebral regions may suggest different functional abilities and mobility patterns. The neonates have spool-shaped vertebrae throughout the vertebrae contrary to the adults. The difference in the size of the centrum and processes is important in the column morphology, and the neonates have no area of vertebral stability. Such a flexible column suggests that they swim slower than adults and still depend on their mothers to feed them. Further research is needed to understand the factors influencing the column/vertebral shape and size between males and females. For now, we can only assume that males and females share the same swimming mode. Sexual size dimorphism may only occur in the cranium of the *Pseudorca*. Overall, the large pod of *Pseudorca* swim together while also taking care of the youngest's. As the *Pseudorca* lives in large mixed pods, when they strand in mass, they provide the opportunity to understand their morphology further as a full growth sequence. Even though the best was done in terms of sampling, the number of specimens studied was limited by time constraints. To have a more homogenous data set, it is advised to include more females, neonates, and fetuses in the study by reaching out to other museums preserving similar specimens.

ACKNOWLEDGMENTS

AUTHOR CONTRIBUTIONS

Mélissa L. Duflot: Conceptualization; data curation; formal analysis; methodology; writing – original draft. **Amandine Gillet:** Writing – review and editing. **Katrina E. Jones:** Writing – review and editing. **Richard Sabin:** Supervision. **Agnese Lanzetti:** Conceptualization; formal analysis; funding acquisition; supervision; writing – review and editing.

ORCID

Mélissa L. Duflot https://orcid.org/0009-0004-5432-565X
Amandine Gillet https://orcid.org/0000-0001-9763-6061
Katrina E. Jones https://orcid.org/0000-0003-1088-0497
Richard Sabin https://orcid.org/0000-0003-0699-7596
Agnese Lanzetti https://orcid.org/0000-0003-1364-0544

REFERENCES

Adams, D. C., Collyer, M. L., & Kaliontzopoulou, A. (2021). *Geomorph: software for geometric morphometric analyses* (R package version 4.0.1) [Computer software]. https://rdocumentation.org/packages/geomorph/versions/4.0.1

Amano, M., & Miyazaki, N. (1996). Geographic variation in external morphology of Dall's porpoise, *Phocoenoides dalli. Aquatic Mammals*, *22*, 167–174.

Baird, R. W. (2018). False killer whale. In B. Würsig, J. G. M. Thewissen, & K. M. Kovacs (Eds.), *Encyclopedia of marine mammals* (3rd ed., pp. 347–349). Academic Press. https://doi.org/10.1016/B978-0-12-804327-1.00006-6

Bardua, C., Felice, R. N., Watanabe, A., Fabre, A.-C., & Goswami, A. (2019). A practical guide to sliding and surface semi-landmarks in morphometric analyses. *Integrative Organismal Biology*, *1*, obz016. https://doi.org/10.1093/iob/obz016

Bateman, N. (1954). Bone growth: a study of the grey-lethal and microphthalmic mutants of the mouse. *Journal of Anatomy*, *88*(2), 212–262.

Bell, C. H., Kemper, C. M., & Conran, J. G. (2002). Common dolphins *Delphinus delphis* in southern Australia: a morphometric study. *Australian Mammalogy*, *24*, 1–10. https://doi.org/10.1071/am02001

Berta, A., & Lanzetti, A. (2020). Feeding in marine mammals: An integration of evolution and ecology through time. *Palaeontologia Electronica*, *23*(2), Article a40. https://doi.org/10.26879/951

Buchholtz, E. A. (2001). Vertebral osteology and swimming style in living and fossil whales (Order: Cetacea). *Journal of Zoology*, *253*(2), 175–190. https://doi.org/10.1017/S0952836901000164

Buchholtz, E. A. (2011). Vertebral and rib anatomy in *Caperea marginata*: Implications for evolutionary patterning of the mammalian vertebral column. *Marine Mammal Science*, *27*(2), 382–397. https://doi.org/10.1111/j.1748-7692.2010.00411.x

Buchholtz, E. A., & Schur, S. A. (2004). Vertebral osteology in Delphinidae (Cetacea). *Zoological Journal of the Linnean Society* *140*, 383–401. https://doi.org/10.1111/j.1096-3642.2003.00105.x

Clementz, M., Goswami, A., Gingerich, P., & Koch, P. (2006). Isotopic records from early whales and sea cows: Contrasting patterns of ecological transition. *Journal of Vertebrate Paleontology*, *26*(2), 355–370. https://doi.org/10.1671/0272-4634(2006)26[355:IRFEWA]2.0.CO;2

Collyer, M. L. & Adams, D. C. (2013). Phenotypic trajectory analysis: Comparison of shape change patterns in evolution and ecology. *Hystrix*, *24*, 75–83. https://doi.org/10.4404/hystrix-24.1-6298

Collyer, M. L. & Adams, D. C. (2021). *RRPP: Linear model evaluation with randomized residuals in a permutation procedure* (v. 1.0) [Computer software]. https://cran.r-project.org/web/packages/RRPP

Coombs, E. J., Clavel, J., Park, T., Churchill, M., & Goswami, A. (2020). Wonky whales: the evolution of cranial asymmetry in cetaceans. *BMC Biology*, *18*(1), Article 86. https://doi.org/10.1186/s12915-020-00805-4

Coombs, E. J., Deaville, R., Sabin, R. C., Allan, L., O'Connell, M., Berrow, S., Smith, B., Brownlow, A., Doeschate, M. T., Penrose, R., Williams, R., Perkins, M. W., Jepson, P. D., & Cooper, N. (2019). What can cetacean stranding records tell

us? A study of UK and Irish cetacean diversity over the past 100 years. *Marine Mammal Science*, *35*(4), 1527–1555. https://doi.org/10.1111/mms.12610

Cotten, P. B., Piscitelli, M. A., McLellan, W. A., Rommel, S. A., Dearolf, J. L., & Pabst, D.A. (2008). The gross morphology and histochemistry of respiratory muscles in bottlenose dolphins, *Tursiops truncatus*. *Journal of Morphology*, *269*(12), 1520–1538. https://doi.org/10.1002/jmor.10668

del Castillo, D. L., Viglino, M., Flores, D. A. & Capozzo, H. L. (2017). Skull ontogeny and modularity in two species of *Lagenorhynchus*: morphological and ecological implications. *Journal of Morphology*, *278*, 203–214. https://doi.org/10.1002/jmor.20629

Felice, R. N., Tobias, J. A., Pigot, A. L., & Goswami, A. (2019). Dietary niche and the evolution of cranial morphology in birds. *Proceedings of the Royal Society B: Biological Sciences*, *286*, Article 20182677. https://doi.org/10.1098/rspb.2018.2677

Fish, F. (1998). Comparative kinematics and hydrodynamics of odontocete cetaceans: morphological and ecological correlates with swimming performance. *Journal of Experimental Biology*, *201*(20), 2867–2877. https://doi.org/10.1242/jeb.201.20.2867

Fish, F., Peacock, J., & Rohr, J. (2003). Stabilization mechanism in swimming odontocete cetaceans by phased movements. *Marine Mammal Science*, *19*(3), 515–528. https://doi.org/10.1111/j.1748-7692.2003.tb01318.x

Galatius, A., Berta, A., Frandsen, M. S., & Goodall, R. N. P. (2011). Interspecific variation of ontogeny and skull shape among porpoises (Phocoenidae). *Journal of Morphology*, *272*(2), 136–148. https://doi.org/10.1002/jmor.10900

Gillet, A., Frédérich, B., & Parmentier, E. (2019). Divergent evolutionary morphology of the axial skeleton as a potential key innovation in modern cetaceans. *Proceedings of the Royal Society B: Biological Sciences*, *286*, Article 20191771. http://doi.org/10.1098/rspb.2019.1771

Jones, K. E. & German, R. Z. (2014). Ontogenetic allometry in the thoracolumbar spine of mammal species with differing gait use. *Evolution & Development*, *16*(2), 110–120. https://doi.org/10.1111/ede.12069

Kasuya, T., & Izumisawa, Y. (1981). *The fishery-dolphin conflict in the Iki Island*. *Japan area* (Report no. MMC-80/02). Report to the U.S. Marine Mammal Commition on Contract NM1533791-7.

Kitchener, D. J., Ross, G. J. B., & Caputi, N. (1990). Variation in skull and external morphology in the False Killer Whale, *Pseudorca crassidens* from Australia, Scotland and South Africa. *Mammalia*, *54*, 119–135. https://doi.org/10.1515/mamm.1990.54.1.119

Klingenberg, C. P. (1996). Multivariate allometry. In L. F. Marcus, M. Corti, A. Loy, G. J. P. Naylor, & D. E. Slice (Eds.), *Advances in morphometrics* (pp. 23–49). Springer. https://doi.org/10.1007/978-1-4757-9083-2_3

Lang, T. G., & Daybell, D. A. (1963). *Porpoise performance tests in a seawater tank* (Technical Report 3063). U. S. Naval Ordinance Test Station, China Lake, CA.

Lighthill, M. J. (1969). Hydrodynamics of aquatic animal propulsion. *Annual Review of Fluid Mechanics*, *1*, 413–446. https://doi.org/10.1146/annurev.fl.01.010169.002213

Lucas, T., & Goswami, A. (2017). *Paleomorph: geometric morphometric tools for paleobiology* (R package version 0.1.4) [Computer software]. https://CRAN.R-project.org/package=paleomorph

Marchesi, M. C., Boy, C. C., Dans, S. L., Mora, M. S., & González-José, R. (2020a). Morphology of the vertebral centra in dolphins from the southwestern South Atlantic: A 3D morphometric approach and functional implications. *Marine Mammal Science*, *36*(2), 548–564. https://doi.org/10.1111/mms.12660

Marchesi, M. C., Mora, M. S., Dans, S. L., Coscarella, M. A. & González-José, R. (2020b). Vertebral morphology in partially sympatric dolphins: A 3D approach. *Frontiers in Marine Science*, *7*. https://doi.org/10.3389/fmars.2020.581762

Marchesi, M. C., Mora, M. S., Dans, S. L., & González-José, R. (2021). Allometry and ontogeny in the vertebral column of Southern Hemisphere dolphins: a 3D morphofunctional approach. *Journal of Mammalian Evolution*, *28*(1), 125–134. https://doi.org/10.1007/s10914-020-09514-9

Mead, J. G. (1975). Anatomy of the external nasal passages and facial complex in the Delphinidae (Mammalia: Cetacea). *Smithsonian Contributions to Zoology*, *207*, 1–72. https://doi.org/10.5479/si.00810282.207

Mesnick, S., & Ralls, K. (2018). Sexual dimorphism. In B. G. Würsig, J. G. M. Thewissen, & K. M. Kovacs (Eds.), *Encyclopedia of marine mammals* (3rd ed., pp. 848–853). Elsevier.

Ngqulana, S. G., Hofmeyr, G. G., & Plön, S. (2017). Sexual dimorphism in long-beaked common dolphins (*Delphinus capensis*) from KwaZulu-Natal, South Africa. *Journal of Mammalogy*, *98*, 1389–1399. https://doi.org/10.1093/jmammal/gyx086

Noren, S. R., Biedenbach, G., & Edwards, E. F. (2006). Ontogeny of swim performance and mechanics in bottlenose dolphins (*Tursiops truncatus*). *Journal of Experimental Biology 209*(23), 4724–4731. https://doi.org/10.1242/jeb.02566

Odell, D. K., & McClune, K. M. (1999). False killer whale *Pseudorca crassidens* (Owen, 1846). In S. H. Ridgway & R. Harrison (Eds.), *Handbook of marine mammals–volume 6: The second book of dolphins and porpoises* (pp. 213–243). Elsevier.

Pabst, D. A. (1990). Axial muscles and connective tissues of the bottlenose dolphin. In S. Leatherwood & R. R. Reeves (Eds.), *The bottlenose dolphin* (pp. 51–67). Academic Press.

Perrin, W. F., & Reilly, S. B. (1984). Reproductive parameters of dolphins and small whales of the family Delphinidae. *Reports of the International Whaling Commission, Special Issue 6*, 97–133.

Purves, P. E., & Pilleri, G. (1978). The functional anatomy and general biology of *Pseudorca crassidens* (Owen) with a review of the hydrodynamics and acoustics in Cetacea. *Investigations on Cetacea*, *9*, 67–227.

Randau, M., Cuff, A. R., Hutchinson, J. R., Pierce, S. E., & Goswami, A. (2016). Regional differentiation of felid vertebral column evolution: a study of 3D shape trajectories. *Organisms Diversity & Evolution*, *17*, 305–319. https://doi.org/10.1007/s13127-016-0304-4

R Core Team. (2021). *R: A language and environment for statistical computing* (Version 4.1.3) [Computer software]. R Foundation for Statistical Computing.

Rommel, S. (1989). Osteology of the bottlenose dolphin. In S. Leatherwood & R. R. Reeves (Eds.), *The bottlenose dolphin* (pp. 29–49). Academic Press.

Rone, B. K., & Pace, R. M., III. (2012). A simple photograph-based approach for discriminating between free-ranging long-finned (*Globicephala melas*) and short-finned (*G. macrorhynchus*) pilot whales off the east coast of the United States. *Marine Mammal Science*, *28*(2), 254–275. https://doi.org/10.1111/j.1748-7692.2011.00488.x

Schlager, S. (2017). Morpho and Rvcg – Shape analysis in R: R-packages for geometric morphometrics, shape analysis and surface manipulations. In G. Zheng, S. Li, & G. Székely (Eds.), *Statistical shape and deformation analysis* (pp. 217–256). Academic Press. https://doi.org/10.1016/B978-0-12-810493-4.00011-0

Stacey, P. J., Leatherwood, S., & Baird, R. W. (1994). *Pseudorca crassidens*. *American Society of Mammalogists*, *456*, 1–6.

Thewissen, J. G. M., Cooper, L. N., George, J. C., & Bajpai, S. (2009). From land to water: the origin of whales, dolphins, and porpoises. *Evolution: Education and Outreach*, *2*(2), 272–288. https://doi.org/10.1007/s12052-009-0135-2

Tenenhaus, A., & Guillemot, V. (2017). *RGCCA: Regularized and sparse generalized canonical correlation analysis for multiblock data* (Version 2.1.2) [Computer software]. https://CRAN.R-project.org/package=RGCCA

Thomas, D. B., Harmer, A. M. T., Giovanardi, S., Holvast, E. J., McGoverin, C. M., & Tenenhaus, A. (2021). Constructing a multiple-part morphospace using a multiblock method. *Methods in Ecology and Evolution*, *14*(1), 65–76. https://doi.org/10.1111/2041-210X.13781

Tolley, K. A., Read, A. J., Wells, R. S., Urian, K. W., Scott, M. D., Irvine, A. B., & Hohn, A. A. (1995). Sexual dimorphism in wild bottlenose dolphins (*Tursiops truncatus*) from Sarasota, Florida. *Journal of Mammalogy*, *76*, 1190–1198. https://doi.org/10.2307/1382611

Vicari, D., Sabin, R. C., Brown, R. P., Lambert, O., & Bianucci, G. (2022). Skull morphological variation in a British stranded population of false killer whale (*Pseudorca crassidens*): a three-dimensional geometric morphometric approach. *Canadian Journal of Zoology*, *100*(2), 119–132. https://doi.org/10.1139/cjz-2021-0112

Videler, J. & Kamermans, P. (1985). Differences between upstroke and downstroke in swimming dolphins. *Journal of Experimental Biology*, *119*(1), 265–274. https://doi.org/10.1242/jeb.119.1.265

Watson, A. G., & Fordyce, R. E. (1993). Skeleton of two minke whales, *Balaenoptera acutorostrata*, stranded on the southeast coast of New Zealand. *New Zealand Natural Sciences*, *20*, 1–14.

Yahn, S. N., Baird, R. W., Mahaffy, S. D., & Robertson, K. M. (2023). Sexually dimorphic characteristics of short-finned pilot whales, false killer whales, pygmy killer whales, and melon-headed whales assessed using fin and body morphometrics from photographs taken at sea. *Marine Mammal Science*, *39*(1), 98–113. https://doi.org/10.1111/mms.12963.

Yahn, S. N., Baird, R. W., Mahaffy, S. D., & Webster, D. L. (2019). How to tell them apart? Discriminating tropical blackfish species using fin and body measurements from photographs taken at sea. *Marine Mammal Science*, *35*(4), 1232–1252. https://doi.org/10.1111/mms.12584

Yamada, M. (1956). An analysis in mass osteology of the false killer whale, *Pseudorca crassidens* (Owen) Part 1. *Okajimas Folia Anatomica Japonica*, *28*(1–6), 451–463.

SUPPORTING INFORMATION

Additional supporting information can be found online in the Supporting Information section at the end of this article.